PERTURBATION ANALYSIS AND FEEDBACK CONTROL OF COMMUNICATION NETWORKS USING STOCHASTIC HYBRID MODELS

Haining Yu *,1 **Christos G. Cassandras** *,1

* *Department of Manufacturing Engineering Boston University, Brookline, MA 02446 USA*

Abstract: Communication networks may be abstracted through Stochastic Fluid Models (SFM) with the node dynamics described by switched flow equations as various events take place, thus giving rise to hybrid automaton models with stochastic transitions. The inclusion of feedback mechanisms complicates these dynamics. In a tandem setting, a typical feedback mechanism is the control of a node processing rate as a threshold-based function of the downstream node's buffer level. The problem considered here is to control the threshold parameters so as to optimize performance metrics involving average workload and system throughput and to show how Infinitesimal Perturbation Analysis (IPA) can be used to analyze congestion propagation through a network and develop gradient estimators of such metrics.

Keywords: Discrete Event Systems, Perturbation Analysis, Hybrid Systems, Communication Networks

1. INTRODUCTION

Fluid models have been long adopted as a modeling technique for communication networks. Introduced in (Anick *et al.*, 1982) and later proposed in (Kobayashi and Ren, 1992) for the analysis of multiplexed data streams and in (Cruz, 1991) for network performance, fluid models have been shown to be especially useful for simulating various kinds of high speed networks (Kesidis *et al.*, 1996),(Kumaran and Mitra, 1998),(Liu *et al.*, 1999). Stochastic Flow Models (SFM) have the extra feature that the flow rates are treated as *stochastic* processes. Under this modelling technique, a new approach for sensitivity analysis has been recently proposed, based on Infinitesimal Perturbation Analysis (IPA) (Liu and Gong, 1999),(Cassandras *et al.*, 2002). The essence of this approach is the on-line estimation of gradients (sensitivities) of certain performance measures with respect to various controllable parameters. These estimates may be incorporated in standard gradient-based algorithms to optimize the parameter settings.

An important feature in today's communication networks is the presence of *feedback* mechanisms. For example, in Random Early Detection (see (Floyd and Jacobson, 1993)), an IP router may send congestion signals to TCP flows by dropping packets and a TCP flow should adjust its window size (and therefore its sending rate) according to feedback signals (for example, acknowledgement packets sent back from a destination node). However, queueing networks have been studied largely based on the assumption that the system state, typically queue length information, has no effect on arrival and service processes, i.e., in the absence of feedback. Unfortunately, the presence of feedback significantly complicates analysis, and makes it extremely difficult to derive closed-form expressions of performance metrics such as average queue length or mean waiting time (unless stringent assumptions are made, e.g., in (Takacs, 1963) and (Pekoz and Joglekar, 2002)), let alone developing analytical schemes for performance optimization. It is equally difficult to ex-

[1] The authors' work is supported in part by the National Science Foundation under Grants EEC-00-88073 and DMI-0330171, by AFOSR under grants FA9550-04-1-0133 and FA9550-04-1-0208, and by ARO under grant DAAD19-01-0610.

tend the theory of PA for discrete-event queueing systems in the presence of feedback.

Motivated by the importance of incorporating feedback to stochastic DES as well as their SFM counterparts, and the effectiveness of IPA methods applied to SFMs to date, we have been applying IPA to SFMs with various feedback mechanisms in (Yu and Cassandras, 2004*c*) and (Yu and Cassandras, 2004*a*). However, the study in (Yu and Cassandras, 2004*c*) and (Yu and Cassandras, 2004*a*) is limited to systems with single queues. (Sun *et al.*, 2003) studies IPA in tandem networks, but no feedback mechanism is employed. This limitation has restricted the use of IPA in practical applications such as computer networks, where feedback may span multiple nodes.

To overcome this restriction, in this paper we extend our earlier work to study the behavior of IPA in a feedback-controlled two-node tandem network. We observe that the system may switch among different modes when certain discrete events occur, and when staying in each mode the system is driven by a set of differential equations. This combination of time-driven and event-driven dynamics is what characterizes *hybrid systems* (see, e.g., (Alur *et al.*, 1996)). Hybrid systems have been found very useful in modelling complex communication networks, e.g., in (Hespanha *et al.*, 2001), where time-driven behaviors (e.g., temperature, speed) and event-driven mechanisms (e.g., human operations) closely interact with each other.

The hybrid nature of the system adds significant difficulty to our analysis. In order to carry out control and optimization tasks, we first construct a stochastic hybrid automaton based on the SFM dynamics and then carry out IPA. The main contributions of the paper are the construction of a stochastic hybrid automaton for control and optimization purposes, and the derivation of IPA gradient estimators for performance metrics such as workload and throughput. Even though the presence of feedback in the SFM considerably complicates the task of carrying out IPA, we are able to obtain such IPA estimators and they depend only on information observable from an actual sample path, making them readily applicable in online control and optimization. It is also worth reiterating that in the SFM we consider in this paper, as well as in (Cassandras *et al.*, 2002) and (Yu and Cassandras, 2004*c*), all flow rates are treated as random processes without distributional assumptions, allows us to capture the randomness in time-varying behavior of the network traffic.

The paper is organized as follows. First in Section 2, we present the feedback-based buffer control problem in the SFM setting. In Section 3 we construct the stochastic hybrid automaton. In Section 4, we carry out IPA by first deriving queue content derivatives in our model and then obtaining the IPA estimators for the gradients of the average workload and throughput with respect to feedback control parameters. Finally in Section 5 we outline a number of open problems and future research directions.

2. STOCHASTIC FLOW MODEL OF A TWO-NODE SYSTEM WITH FEEDBACK

The SFM of a two-node network is shown in Fig. 1. Each node has infinite capacity and the buffer content at time t is $x_n(t)$. When buffers have finite capacity, it will become clear that our analysis proceeds along the same lines with additional states defined in the hybrid automaton model. For node $n = 1, 2$, we denote the incoming flow rate by $\alpha_n(t)$, the service rate by $\beta_n(t)$, and the outgoing flow rate by $\delta_n(t)$ where $\delta_1(t) = \alpha_2(t)$.

In a network composed of multiple nodes, congestion often arises and the purpose of a feedback control policy is to alleviate it by appropriately reducing the incoming traffic at the congested node. The simplest way is to use queue content information at nodes. In the system of Fig. 1, a controller is used to throttle the outflow rate of node 1 as the buffer level in node 2 increases. However, continuously monitoring buffer levels is impractical, as it requires that node 2 continuously supplies buffer level information to node 1, which involves a large amount of communication overhead coupled with the issue of delayed information arriving at node 1. Thus, a more efficient quantized feedback control policy is chosen as follows: Node 1 can process the incoming flow in two modes: in the *high* mode the service rate is $\beta_{1\max}(t)$; in the *low* mode it is $\beta_{1\min}(t)$. When $x_2(t) < \phi$ for some given parameter $\phi > 0$, node 1 is in the high mode and $\beta_1(t) = \beta_{1\max}(t)$; when the buffer content of node 2 becomes too high, i.e., $x_2(t) > \phi$, node 1 switches to the low mode and $\beta_1(t) = \beta_{1\min}(t)$. We assume that $\beta_{1\min}(t)$ and $\beta_{1\max}(t)$ are both time-varying functions, and $\beta_{1\min}(t) \leq \beta_{1\max}(t)$ w.p.1. In this system, the defining processes are $\alpha_1(t), \beta_{1\min}(t), \beta_{1\max}(t), \beta_2(t)$, which are all independent of the system state, system parameters or other defining processes. We make the following *Assumption 1: All defining processes $\alpha_1(t), \beta_{1\min}(t), \beta_{1\max}(t), \beta_2(t)$ are bounded w.p.1 and piecewise constant; moreover, at any time t, any two of them are not equal to each other w.p.1.*

Clearly, the service rate (and consequently the outgoing flow rate) of node 1 is dependent on the queue content of node 2 as follows:

$$\beta_1(t) = \begin{cases} \beta_{1\max}(t) & \text{when } x_2(t) < \phi \\ \beta_2(t) & \text{when } x_2(t) = \phi \text{ and} \\ & \beta_{1\min}(t) \leq \beta_2(t) \leq \beta_{1\max}(t) \\ \beta_{1\min}(t) & \text{otherwise} \end{cases} \tag{1}$$

where the second case is a consequence of feedback and it captures the chattering behavior of the actual system when $x_2(t) = \phi$ and $\beta_{1\min}(t) \leq \beta_2(t) \leq \beta_{1\max}(t)$. Note that it is impossible for the state $(x_1(t), x_2(t)) = (0, \phi)$ to exist for any finite period of time. The reason is that $x_1(t) = 0$ implies $\alpha_2(t) = \delta_1(t) = \alpha_1(t)$ and $x_2(t) = \phi$

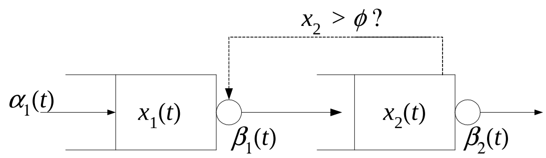

Fig. 1. SFM of 2-node system with feedback

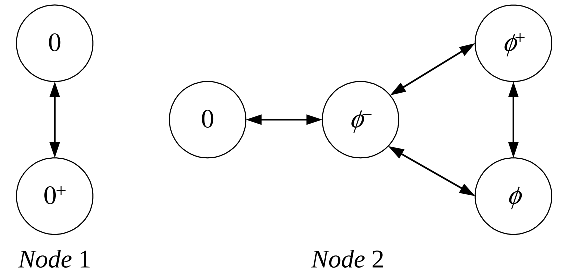

Fig. 2. State transition diagram of the two nodes

implies $\alpha_2(t) = \beta_2(t)$; however, $\alpha_1(t) = \beta_2(t)$ is excluded by Assumption 1.

We are now able to provide the system dynamics for $n = 1, 2$:

$$\frac{dx_n(t)}{dt^+} = \begin{cases} 0 & \text{if } x_n(t) = 0 \text{ and} \\ & \alpha_n(t) - \beta_n(t) \le 0 \\ \alpha_n(t) - \beta_n(t) & \text{otherwise} \end{cases} \tag{2}$$

The outflow rate is given by

$$\delta_n(t) = \begin{cases} \alpha_n(t) & \text{if } x_n(t) = 0 \text{ and} \\ & \alpha_n(t) - \beta_n(t) \le 0 \\ \beta_n(t) & \text{otherwise} \end{cases} \tag{3}$$

and note that $\delta_n(t) \le \beta_n(t)$. Finally, observe that, because of the presence of feedback, the dynamics of $x_1(t)$ and $x_2(t)$ are strongly coupled. This is the critical difference between our work and the work in (Sun *et al.*, 2003).

3. THE STOCHASTIC HYBRID AUTOMATON MODEL

3.1 Sample Path Decomposition

The SFM dynamics presented in the last section provide a detailed description of the system. In this section we establish a stochastic hybrid automaton model based on an abstraction process. In particular, we decompose a typical sample path into different intervals. The state trajectory of node 1 can be decomposed into the intervals during which $x_1(t) = 0$, and the intervals during which $x_1(t) > 0$. Accordingly, we identify two *aggregate states* for node 1, denoted by 0 and 0^+ respectively. Each aggregate state, denoted by $s_1(t) \in \{0, 0^+\}$, corresponds to one class of intervals and we impose the ordering relationship $0 < 0^+$. For node 2, there are two critical thresholds, 0 and ϕ, and the sample path of node 2 can be similarly decomposed into four kinds of intervals: the intervals during which $x_2(t) = 0$ with an aggregate state $s_2(t) = 0$, the intervals during which $0 < x_2(t) < \phi$ with $s_2(t) = \phi^-$, the intervals during which $x_2(t) = \phi$ with $s_2(t) = \phi$, and the intervals during which $x_2(t) > \phi$ with $s_2(t) = \phi^+$. The aggregate state ordering we impose is $0 < \phi^- < \phi < \phi^+$.

Let us use $s(t) = (s_1(t), s_2(t))$ to denote the aggregate state of the system. An *aggregate state transition* occurs when the value of $s(t)$ changes, corresponding to an aggregate state change in one or more nodes. Fig. 2 shows the state transitions for each node.

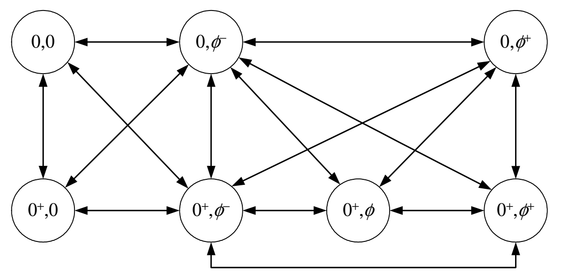

Fig. 3. Hybrid automaton with all possible transitions

As mentioned earlier, $(0, \phi)$ is impossible. Hence, we get $s(t) \in \{(0,0), (0,\phi^-), (0,\phi^+), (0^+,0), (0^+,\phi^-), (0^+,\phi), (0^+,\phi^+)\}$. Fig. 3 shows the hybrid automaton with all possible state transitions for the system. If $s_1(t)$ remains constant, the state transition is shown as a *horizontal* edge. If $s_2(t)$ remains constant, the state transition is shown as a *vertical* edge. If both $s_1(t)$ and $s_2(t)$ change, the transition is shown as a *diagonal* edge.

We are interested in the underlying events which cause state transitions to occur. These events can be classified into two categories: an *exogenous* event is defined as a switch in any of the defining processes; an *endogenous* event occurs when the buffer level of either node reaches a critical value, i.e., 0 for node 1, and 0 or ϕ for node 2. We also make the following *Assumption 2*: *W.p. 1, no two (endogenous or exogenous) events occur at the same time.* Note that not all transitions are feasible and the task of the next section is to discuss their feasibility.

3.2 Identifying Feasible State Transitions

In this section we check for infeasible state transitions so as to trim the edges of the transition diagram in Fig. 3. Let us assume a state transition occurs at time π. We use (s_1, s_2) to denote the aggregate state of the system before π and (σ_1, σ_2) to denote the aggregate state after π. Any transition in Fig. 3 falls into one of the following three categories: (*i*) $s_1 = \sigma_1$ and $s_2 \neq \sigma_2$, (*ii*) $s_1 \neq \sigma_1$ and $s_2 = \sigma_2$, and (*iii*) $s_1 \neq \sigma_1$ and $s_2 \neq \sigma_2$. In Fig. 3, the transitions in the above three categories are shown as vertical, horizontal and diagonal edges respectively. Regarding their feasibility, first we point out that every transition in the first two categories is possible since it corresponds to a state transition in an isolated node. Second, according to Assumption 2, no two endogenous events occur at the same time. Therefore, the diagonal state transitions $(0^+, \phi^-) \to (0, 0)$, $(0^+, \phi^+) \to (0, \phi^-)$, and $(0^+, \phi^-) \to (0, \phi^+)$ are infeasible. Finally, in the next lemma, we prove that an additional class of diagonal transitions is infeasible (all proofs are omitted but may be found in (Yu and Cassandras, 2004*b*)).

Lemma 1. Assume an endogenous transition $(s_1, s_2) \to (\sigma_1, \sigma_2)$ occurs at time π such that $s_1 \neq \sigma_1$ and $s_2 \neq \sigma_2$. The transition is infeasible if (*i*) $s_1 > \sigma_1$ and $s_2 < \sigma_2$, or (*ii*) $s_1 < \sigma_1$ and $s_2 > \sigma_2$.

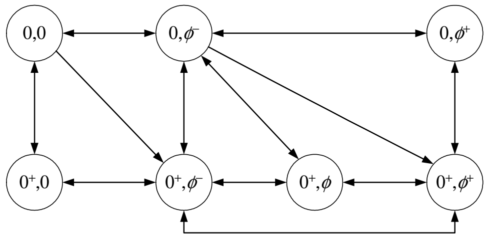

Fig. 4. Hybrid automaton with feasible transitions

The remaining transitions are all feasible and the resulting hybrid automaton is shown in Fig. 4. To summarize, we have established a *stochastic hybrid automaton model*, where the nodes represent aggregate states of the SFM, the edges represent transitions or events, and the continuous dynamics in each aggregate state are given by (2) and (1). We will soon realize the importance of this stochastic hybrid automaton as we carry out Infinitesimal Perturbation Analysis (IPA) for control and optimization tasks in the next section.

4. IPA FOR QUEUE CONTENT DERIVATIVES

In this section we carry out IPA to study the effect of the controllable parameter ϕ on the system state $(x_1(t), x_2(t))$ from which we can deduce performance sensitivity estimates as discussed in Section 5. For node $n = 1, 2$, we will use the notation $x'_n(t) \equiv \partial x_n(t;\phi)/\partial\phi$. Note that $x'_n(t)$ is a piecewise constant function. According to the system dynamics in (2), between two consecutive state transitions, the system dynamics for node n are completely decided by $\alpha_n(t)$ and $\beta_n(t)$. Recall that over such an interval $\alpha_n(t)$ is fixed to a single defining process $\alpha_1(t), \beta_{1\max}(t), \beta_{1\min}(t)$ or $\beta_2(t)$, so it is locally independent of ϕ. The same argument applies to $\beta_n(t)$. Therefore, $x'_n(t)$ remains constant between two consecutive transitions. However, when a state transition occurs, $x'_n(t)$ may jump from one value to another. In other words, $x'_n(t)$ changes only when an event triggers a state transition in the hybrid automaton in Fig. 4. This section is devoted to the study of the evolution of queue content derivatives when these transitions occur. Let us assume a state transition takes place at time π. Then, $x'_1(\pi^+)$ and $x'_2(\pi^+)$ may depend on the value $x'_2(\pi^-)$ and $x'_2(\pi^-)$. If the value of $x'_2(\pi^+)$ depends on the value of $x'_1(\pi^-)$, we call this phenomenon *downstream propagation* of a queue content perturbation; if $x'_1(\pi^+)$ depends on the value of $x'_2(\pi^-)$, we refer to it as *upstream propagation*. Downstream propagation was observed in (Sun *et al.*, 2003) for tandem networks with no feedback; upstream propagation, however, was not present because of the absence of feedback.

In the remaining of this section, we are going to study the dynamics of $x'_n(t)$ when an arbitrary state transition $(s_1, s_2) \to (\sigma_1, \sigma_2)$ occurs.

4.1 State Transitions in Node 1 Only (Vertical Transitions)

We begin with IPA for vertical state transitions, i.e., transitions of the form $(s_1, s_2) \to (\sigma_1, s_2)$. It follows that $\beta_1(t)$ is equal to a fixed defining process and no upstream propagation may take place in this case, consistent with the results in (Sun *et al.*, 2003).

Lemma 2. If a transition $(s_1, s_2) \to (\sigma_1, s_2)$ occurs, we get $x'_1(\pi^+) = 0$ and

$$x'_2(\pi^+) = \begin{cases} x'_2(\pi^-) + x'_1(\pi^-) & \text{if } \sigma_1 = 0 \\ & \text{and } s_2 > 0 \\ x'_2(\pi^-) & \text{otherwise} \end{cases}$$

4.2 State Transitions in Node 2 Only (Horizontal Transitions)

Next we consider transitions of the form $(s_1, s_2) \to (s_1, \sigma_2)$. Since $\beta_1(t)$ depends on $x_2(t)$, upstream propagation is expected when horizontal transitions take place and certain conditions are met. In what follows, we classify all horizontal transitions into three classes and discuss them case by case.

Case 1: If $s_1 = 0$, no upstream propagation may take place. This applies to transitions $(0, 0) \to (0, \phi^-)$, $(0, \phi^-) \to (0, 0)$, $(0, \phi^-) \to (0, \phi^+)$, and $(0, \phi^+) \to (0, \phi^-)$. The complete perturbation dynamics are given by the following result.

Lemma 3. If a transition $(0, s_2) \to (0, \sigma_2)$ occurs, we get $x'_1(\pi^+) = 0$ and

$$x'_2(\pi^+) = \begin{cases} 0 & \text{if } x_2(\pi) = 0 \\ x'_2(\pi^-) & \text{otherwise} \end{cases}$$

Case 2: If $s_2 < \phi$ and $\sigma_2 < \phi$, $\beta_1(t)$ is unaffected by ϕ and no feedback occurs which prevents any perturbation propagation. This applies to transitions $(0, 0) \to (0, \phi^-), (0, \phi^-) \to (0, 0), (0^+, 0) \to (0^+, \phi^-)$ and $(0^+, \phi^-) \to (0^+, 0)$.

Lemma 4. If a transition $(s_1, s_2) \to (s_1, \sigma_2)$ occurs such that $s_2 = 0$ or $\sigma_2 = 0$, we get $x_1(\pi^+) = x_1(\pi^-)$ and $x_2(\pi^+) = 0$

Case 3: If $x_1(\pi) > 0$ (thus its outflow rate is $\beta_1(t)$) and $x_2(\pi) = \phi$, $\beta_1(t)$ switches from one defining process to another. In this case, upstream propagation is expected to take place. Note that for the two-node system, $\frac{d}{dt}[x_1(t) + x_2(t)] = [\alpha_1(t) - \beta_1(t)] + [\beta_1(t) - \beta_2(t)] = \alpha_1(t) - \beta_2(t)$ as long as $x_2(t) > 0$. It follows that $x'_1(t) + x'_2(t)$ remains constant. Specifically, during the state transition we have the following useful relationship

$$x'_1(\pi^+) + x'_2(\pi^+) = x'_1(\pi^-) + x'_2(\pi^-) \quad (4)$$

The perturbation dynamics in Case 3 are described in the following two lemmas.

Lemma 5. If a transition $(0^+, s_2) \to (0^+, \sigma_2)$ occurs such that $s_2 = \phi$ or $\sigma_2 = \phi$, we get $x'_1(\pi^+) = x'_1(\pi^-) + x'_2(\pi^-) - 1$ and $x'_2(\pi^+) = 1$.

This result applies to transitions $(0^+,\phi^-) \to (0^+,\phi),(0^+,\phi) \to (0^+,\phi^-),(0^+,\phi) \to (0^+,\phi^+)$ and $(0^+,\phi^+) \to (0^+,\phi)$. In this case, we can see that upstream propagation exists. Moreover, $x_2'(\pi^+) = 1$ implies a perturbation of magnitude 1 (but with opposite sign) is generated at both nodes.

Lemma 6. If a transition $(0^+, s_2) \to (0^+, \sigma_2)$ occurs such that (i) $s_2 = \phi^-$ and $\sigma_2 = \phi^+$ or (ii) $s_2 = \phi^+$ and $\sigma_2 = \phi^-$, we get

$$\begin{aligned} x_1'\left(\pi^+\right) &= x_1'\left(\pi^-\right) + \frac{\beta_1\left(\pi^-\right) - \beta_1\left(\pi^+\right)}{\beta_1\left(\pi^-\right) - \beta_2} x_2'\left(\pi^-\right) \\ &\quad + \frac{\beta_1\left(\pi^+\right) - \beta_1\left(\pi^-\right)}{\beta_1\left(\pi^-\right) - \beta_2} \\ x_2'(\pi^+) &= \frac{\beta_1\left(\pi^+\right) - \beta_2}{\beta_1\left(\pi^-\right) - \beta_2} x_2'\left(\pi^-\right) \\ &\quad + \frac{\beta_1\left(\pi^-\right) - \beta_1\left(\pi^+\right)}{\beta_1\left(\pi^-\right) - \beta_2} \end{aligned}$$

where

$$\beta_1\left(\pi^-\right) = \begin{cases} \beta_{1\max}\left(\pi^-\right) & \text{if } x_2\left(\pi^-\right) < \phi \\ \beta_{1\min}\left(\pi^-\right) & \text{if } x_2\left(\pi^-\right) > \phi \end{cases}$$

$$\beta_1\left(\pi^+\right) = \begin{cases} \beta_{1\min}\left(\pi^-\right) & \text{if } x_2\left(\pi^-\right) < \phi \\ \beta_{1\max}\left(\pi^-\right) & \text{if } x_2\left(\pi^-\right) > \phi \end{cases}$$

This result applies to transitions $(0^+,\phi^-) \to (0^+,\phi^+)$ and $(0^+,\phi^+) \to (0^+,\phi^-)$. Similar to the previous case, upstream propagation exists and a perturbation of magnitude $\frac{\beta_1(\pi^+)-\beta_1(\pi^-)}{\beta_1(\pi^-)-\beta_2}$ is generated at both nodes.

4.3 Simultaneous State Transitions in Both Nodes (Diagonal Transitions)

Finally, let us focus on the four remaining diagonal transitions.

1. Transition $(0,0) \to (0^+,\phi^-)$. This is an exogenous event, i.e., $\partial\pi/\partial\phi = 0$. Therefore $x_1'(\pi^-) = x_1'(\pi^+) = x_2'(\pi^-) = x_2'(\pi^+) = 0$. Thus, perturbations in both nodes remain constant and there is no upstream or downstream propagation.

2. Transition $(0,\phi^-) \to (0^+,\phi)$. This is an endogenous event. Since $\sigma_2 = \phi$, we have $x_2'(\pi^+) = 1$. Moreover, since $s_2 = \phi^-$ and $\sigma_2 = \phi$, $x_2(\pi) > 0$. Therefore (4) holds. It follows that

$$\begin{aligned} x_1'(\pi^+) &= x_1'(\pi^-) + x_2'(\pi^-) - x_2'\left(\pi^+\right) \\ &= x_2'(\pi^-) - 1 \end{aligned}$$

In this case, we observe upstream propagation and perturbation generation in both nodes.

3. Transition $(0^+,\phi) \to (0,\phi^-)$. Since $x_1(\pi^+) = 0$, we get $x_1'(\pi^+) = 0$. Recalling (4), we also get

$$\begin{aligned} x_2'(\pi^+) &= x_1'(\pi^-) + x_2'(\pi^-) - x_1'(\pi^+) \\ &= x_1'\left(\pi^-\right) + 1 \end{aligned}$$

Thus, both downstream propagation and perturbation generation at node 2 take place.

4. Transition $(0,\phi^-) \to (0^+,\phi^+)$. For $t < \pi$ at node 2, we have

$$x_2(\pi) = \phi = x_2(t) + \int_t^\pi \left[\alpha_1(\tau) - \beta_2(\tau)\right] d\tau$$

It follows that

$$1 = x_2'(\pi^-) + [\alpha_1 - \beta_2]\frac{\partial \pi}{\partial \phi}$$

which gives

$$\frac{\partial \pi}{\partial \phi} = \frac{1 - x_2'(\pi^-)}{\alpha_1 - \beta_2}$$

Moreover, for $t_0 < \pi < t_1$,

$$\begin{aligned} x_2(t_1) = x_2(t_0) &+ \int_{t_0}^\pi \left[\alpha_1(\tau) - \beta_2(\tau)\right] d\tau \\ &+ \int_\pi^{t_1} \left[\beta_{1\min}(\tau) - \beta_2(\tau)\right] d\tau \end{aligned}$$

It follows that

$$\begin{aligned} x_2'(\pi^+) &= x_2'(\pi^-) + [\alpha_1 - \beta_{1\min}]\frac{1 - x_2'(\pi^-)}{\alpha_1 - \beta_2} \\ &= \frac{\beta_{1\min} - \beta_2}{\alpha_1 - \beta_2} x_2'(\pi^-) + \frac{\alpha_1 - \beta_{1\min}}{\alpha_1 - \beta_2} \end{aligned}$$

Recalling (4), we also get

$$\begin{aligned} x_1'(\pi^+) &= x_1'(\pi^-) + x_2'(\pi^-) - x_2'(\pi^+) \\ &= \frac{\alpha_1 - \beta_{1\min}}{\alpha_1 - \beta_2} x_2'(\pi^-) + \frac{\beta_{1\min} - \alpha_1}{\alpha_1 - \beta_2} \end{aligned}$$

Hence, only upstream propagation occurs and there is perturbation generation at both nodes.

5. IPA FOR PERFORMANCE METRICS

So far we have carried out IPA for the queue content derivatives. In this section we present IPA estimators for certain performance metrics. In particular, we define the *Average Workload* for each node $n = 1,2$ as

$$Q_T^n = \frac{1}{T}\int_0^T x_n(t)dt,$$

and the *System Throughput* as

$$H_T = \frac{1}{T}\int_0^T \delta_2(t)dt.$$

Let us use $\pi_i, i = 0,...,I$ to denote the ith state transition event in the time interval $[0,T]$, where I is the number of events. For notational consistency we also define $\pi_0 = 0$ and $\pi_I = T$.

For the workload we get:

$$Q_T^n = \frac{1}{T}\sum_{i=0}^{I-1}\int_{\pi_i}^{\pi_{i+1}} x_n(t)dt$$

After some technical details (see (Yu and Cassandras, 2004b)) it follows that

$$\frac{dQ_T^n}{d\phi} = \int_0^T x_n'(t)dt$$

In other words, the IPA estimator for the average workload is the integral of the queue content derivative. Note that, the result in Section 3 shows that $x_n'(t)$ is piecewise constant. Therefore we get

$$\frac{dQ_T^n}{d\phi} = \sum_{i=0}^{I-1} (\pi_{i+1} - \pi_i) x_n'(\pi_i^+). \tag{5}$$

In summary, the IPA estimator for the average workload requires only (i) the update of queue content sample derivative, which has been discussed in detail in Section 3, and (ii) a timer to record the length of the time interval between two consecutive state transition events.

Similarly the IPA estimator for throughput can be established. Again the derivation is omitted and can be found in (Yu and Cassandras, 2004*b*).

$$\frac{dH_T}{d\phi} = \sum_{i=0}^{I-1} \left[\delta_2(\pi_i^-) - \delta_2(\pi_i^+)\right] \frac{\partial \pi_i}{\partial \phi} \tag{6}$$

where

$$\frac{\partial \pi_i}{\partial \phi} = \begin{cases} 0 & \text{if event at } \pi_i \text{ is exogenous} \\ \frac{\frac{\partial x_n(\pi_i)}{\partial \phi} - x_n'(\pi_i^-)}{\alpha_n(\pi_i^-) - \beta_n(\pi_i^-)} & \text{otherwise} \end{cases}$$

and $n \in \{1, 2\}$ is the node whose buffer level reaches the critical value at time π_i when the event is endogenous, and

$$\frac{\partial x_n(\pi_i)}{\partial \phi} = \begin{cases} 1 & \text{if } n = 2 \text{ and } x_2(\pi_i) = \phi \\ 0 & \text{otherwise} \end{cases}$$

6. CONCLUSIONS AND FUTURE WORK

SFMs have recently been used to capture the dynamics of complex stochastic discrete event systems in order to implement control and optimization methods based on IPA-based gradient estimates. In this paper, we have extended our earlier work in (Yu and Cassandras, 2004*c*) and (Yu and Cassandras, 2004*a*) and further explored the effect of feedback by considering a two-node SFM with some inter-node feedback mechanism. The presence of feedback greatly complicated the analysis by strongly coupling the dynamics of the two nodes. To overcome this difficulty, we have established a hybrid stochastic automaton model for the SFM and achieved IPA estimators for workload and throughput related performance metrics.

The work in this paper opens up a variety of possible extensions. First, it is interesting to study unbiasedness of IPA estimators (5) and (6) in the presence of inter-node feedback. Next, the strong coupling nature of this SFM forces the dimensionality of the stochastic hybrid automaton diagram to become very large as the number of nodes increases. However, our results do date show that an automated construction of the stochastic hybrid automaton is still possible. Finally, the assumption of infinite buffer capacity was made mainly for analytical simplicity. We believe that removing this assumption will add no conceptual obstacles to the analysis.

REFERENCES

Alur, A., Henzinger, T. A. and Sontag, E. D., Eds.) (1996). *Hybrid Systems*. Springer-Verlag.

Anick, D., D. Mitra and M. M. Sondhi (1982). Stochastic theory of a data-handling system with multiple sources. *The Bell System Technical Journal* **Vol. 61**, 1871–1894.

Cassandras, C. G., Y. Wardi, B. Melamed, G. Sun and C. G. Panayiotou (2002). Perturbation analysis for online control and optimization of stochastic fluid models. *IEEE Transactions on Automatic Control* **47**(8), 1234–1248.

Cruz, R. L. (1991). A calculus for network delay, Part I: Network elements in isolation. *IEEE Transactions on Information Theory.*

Floyd, S. and V. Jacobson (1993). Random early detection gateways for congestion avoidance. *IEEE/ACM Transactions on Networking* **1**, 397–413.

Hespanha, João P., Stephan Bohacek, Katia Obraczka and Junsoo Lee (2001). Hybrid modeling of TCP congestion control. In: *Hybrid Systems: Computation and Control, No. 2034 in Lecture Notes in Computer Science* (Maria Domenica Di Benedetto and Alberto Sangiovanni-Vincentelli, Eds.). pp. 291–304.

Kesidis, G., A. Singh, D. Cheung and W.W. Kwok (1996). Feasibility of fluid-driven simulation for ATM network. In: *Proceedings of IEEE Globecom*. Vol. 3. pp. 2013–2017.

Kobayashi, H. and Q. Ren (1992). A mathematical theory for transient analysis of communications networks. *IEICE Transactions on Communications* **E75-B**, 1266–1276.

Kumaran, K. and D. Mitra (1998). Performance and fluid simulations of a novel shared buffer management system. In: *Proceedings of IEEE INFOCOM.*

Liu, B., Y. Guo, J. Kurose, D. Towsley and W. B. Gong (1999). Fluid simulation of large scale networks: Issues and tradeoffs. In: *Proceedings of the International Conference on Parallel and Distributed Processing Techniques and Applications*. Las Vegas, Nevada.

Liu, Y. and W. B. Gong (1999). Perturbation analysis for stochastic fluid queueing systems. In: *Proceedings of the 38th IEEE Conference on Decision and Control*. pp. 4440–4445.

Pekoz, E. and N. Joglekar (2002). Poisson traffic flow in a general feedback queue. *Journal of Applied Probability* **39**, 630–636.

Sun, G., C. G. Cassandras, Y. Wardi and C. G. Panayiotou (2003). Perturbation analysis of stochastic flow networks. In: *Proceedings of the 42th IEEE Conference On Decision and Control*. pp. 4831–4836.

Takacs, L. (1963). A single-server queue with feedback. *Bell System Technical Journal* **42**, 505–519.

Yu, H. and C. G. Cassandras (2004*a*). Multiplicative feedback control in communication networks using stochastic flow models. In: *43th IEEE Conference on Decision and Control*. accepted.

Yu, H. and C. G. Cassandras (2004*b*). Perturbation analysis and feedback control of communication networks using stochastic hybrid models. Technical report. Boston Univ., Dept of Manuf. Eng. . See also http://vita.bu.edu/cgc/Fullpubs/TR04.pdf.

Yu, H. and C. G. Cassandras (2004*c*). Perturbation analysis of feedback-controlled stochastic flow systems. *IEEE Transactions on Automatic Control* **49**(8), 1317–1332.